ACCOUNTS
of chemical research

Evolution of Strategies for Modern Rechargeable Batteries

JOHN B. GOODENOUGH*

Virginia H. Cockrell Centennial Chair in Engineering, Departments of Mechanical Engineering and Electrical & Computer Engineering, The University of Texas at Austin, Engineering Teaching Center II (ETC), 204 East Dean Keeton Street, Austin, Texas 78712, United States

RECEIVED ON OCTOBER 26, 2011

CONSPECTUS

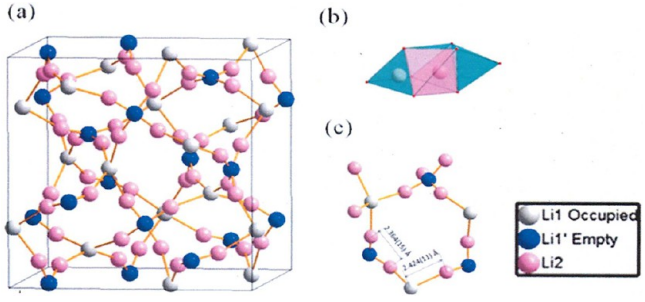

This Account provides perspective on the evolution of the rechargeable battery and summarizes innovations in the development of these devices. Initially, I describe the components of a conventional rechargeable battery along with the engineering parameters that define the figures of merit for a single cell. In 1967, researchers discovered fast Na^+ conduction at 300 K in Na β,β''-alumina. Since then battery technology has evolved from a strongly acidic or alkaline aqueous electrolyte with protons as the working ion to an organic liquid-carbonate electrolyte with Li^+ as the working ion in a Li-ion battery. The invention of the sodium-sulfur and Zebra batteries stimulated consideration of framework structures as crystalline hosts for mobile guest alkali ions, and the jump in oil prices in the early 1970s prompted researchers to consider alternative room-temperature batteries with aprotic liquid electrolytes. With the existence of Li primary cells and ongoing research on the chemistry of reversible Li intercalation into layered chalcogenides, industry invested in the production of a Li/TiS_2 rechargeable cell. However, on repeated recharge, dendrites grew across the electrolyte from the anode to the cathode, leading to dangerous short-circuits in the cell in the presence of the flammable organic liquid electrolyte. Because lowering the voltage of the anode would prevent cells with layered-chalcogenide cathodes from competing with cells that had an aqueous electrolyte, researchers quickly abandoned this effort. However, once it was realized that an oxide cathode could offer a larger voltage versus lithium, researchers considered the extraction of Li from the layered $LiMO_2$ oxides with M = Co or Ni.

These oxide cathodes were fabricated in a discharged state, and battery manufacturers could not conceive of assembling a cell with a discharged cathode. Meanwhile, exploration of Li intercalation into graphite showed that reversible Li insertion into carbon occurred without dendrite formation. The SONY corporation used the $LiCoO_2$/carbon battery to power their initial cellular telephone and launched the wireless revolution. As researchers developed 3D transition-metal hosts, manufacturers introduced spinel and olivine hosts in the $Li_x[Mn_2]O_4$ and $LiFe(PO_4)$ cathodes. However, current Li-ion batteries fall short of the desired specifications for electric-powered automobiles and the storage of electrical energy generated by wind and solar power. These demands are stimulating new strategies for electrochemical cells that can safely and affordably meet those challenges.

1. Evolution of Strategies for Modern Rechargeable Batteries

Introduction[1]**.** Achieving a secure and sustainable energy supply for all people is, perhaps, the greatest technical and societal challenge of our time. Civilization must find a way to reduce the imprint on air pollution of the internal combustion engine and to generate and store efficiently electrical energy generated by solar and/or wind power with an affordable technology. The rechargeable battery and the electrochemical capacitor together can be a

Published on the Web 07/02/2012 www.pubs.acs.org/accounts
10.1021/ar2002705

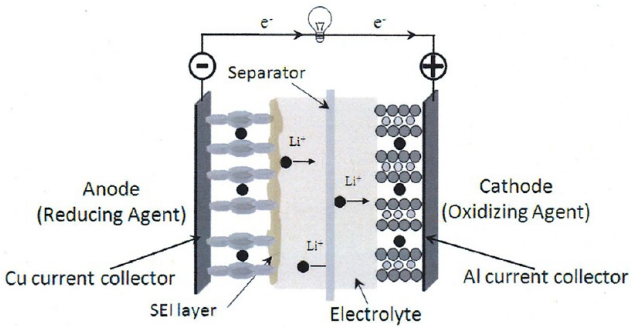

FIGURE 1. Representation of the C/$LiCoO_2$ cell.

portable or stationary store of electric power; but at what cost? At what energy and power density? For how long and how safely?

A battery is made up of one or more interconnected cells. The output current I and/or time Δt to depletion of the stored energy can be increased by connecting cells in parallel; the voltage V for a desired power $P = IV$ by connecting cells in series. Here, we address only issues related to strategies for individual rechargeable battery cells.

2. Electrochemical Cells

An electrochemical cell[2] (see Figure 1) consists of two electrodes, the *anode* and the *cathode*, separated by an *electrolyte*. Solid electrodes separated by a liquid electrolyte are kept apart by an *electrolyte-permeable separator*. The chemical reaction between the anode and the cathode has an electronic and an ionic component. The electrolyte conducts the ionic component, referred to as the *working ion*, inside the cell, but it forces the electronic component to traverse an external electronic circuit. *Current collectors* at the anode and the cathode deliver the electronic current of large-area electrodes to/from *posts* that connect to the external circuit. If the external circuit is disrupted (*open circuit*), the working ion moves inside the cell, but it is not charge-compensated by electrons, so the cathode becomes positively charged and the anode negatively charged until the electrochemical potentials in the two electrodes become equal.

On *discharge*, electrons and ions flow from the anode to the cathode; during *charge*, electrons and ions are forced by an applied electric field to flow from the cathode to the anode. During discharge, an internal resistance R_b to the ionic current I_i reduces the output voltage V_{dis} of a cell relative to the open-circuit voltage V_{oc} by a polarization $\eta = I_i R_b$ (see Figure 2a); the voltage V_{ch} required to charge the cell is increased by η, which then represents an *overvoltage*.

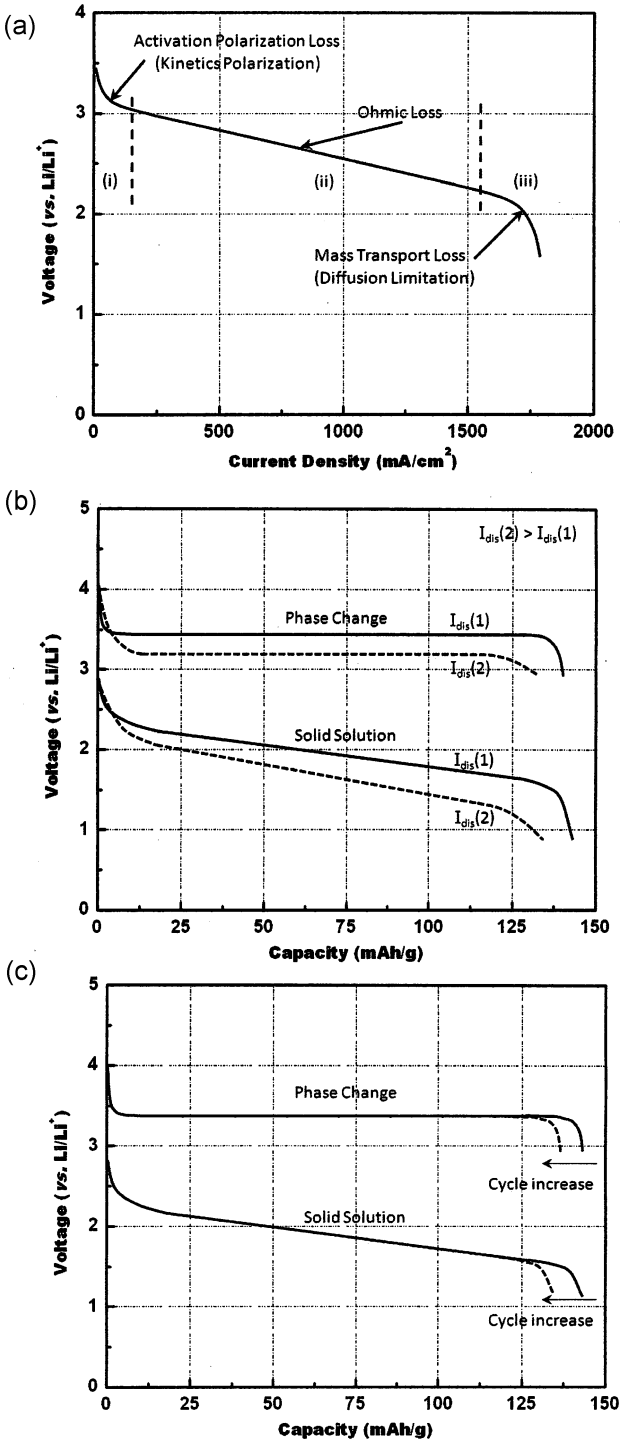

FIGURE 2. (a) Typical V versus I curve. Loss $\eta(i)$ from the resistance to Li^+-ion transport across interfaces, (ii) from the resistance to ionic current in the electrolyte, and (iii) from slow diffusion of the working ion within the host electrode. (b) Typical V versus t or q curves for fixed I_{dis}. *Note:* A flat section in region (ii) signals the presence of a two-phase reaction (Gibbs phase rule). (c) Typical capacity fade; cycle life terminates at 80% of the initial reversible capacity.

Therefore, the discharge and charge voltages of a cell are

$$V_{dis} = V_{oc} - \eta(q, I_{dis}) \qquad (1.1)$$

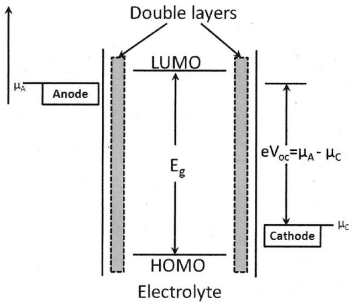

FIGURE 3. Relative energies of μ_A and μ_C versus the LUMO–HOMO window of the electrolyte; $V_{oc} = (\mu_A - \mu_C)/e$, where e is the magnitude of the electron charge.

$$V_{ch} = V_{oc}(q, I_{ch}) + \eta(q, I_{ch}) \tag{1.2}$$

where q represents the state of charge and I_{dis}, I_{ch} are, respectively, the discharge and charge currents. The percent efficiency of a cell to store energy at a fixed current is

$$100 \times \int_0^Q V_{dis}(q)\, dq \Big/ \int_0^Q V_{ch}(q)\, dq \tag{2.0}$$

$$Q = \int_0^{\Delta t} I\, dt = \int_0^Q dq \tag{3.0}$$

where Q is the total charge transferred by the current $I = dq/dt$ on discharge or charge. Q is referred to as the cell *capacity*; it depends on I because the rate of transfer of ions across electrode–electrolyte interfaces becomes diffusion-limited at high currents (Figure 2b). Moreover, on charge/discharge cycling, changes in electrode volume, electrode–electrolyte chemical reactions, and/or electrode decomposition can cause an *irreversible loss* of capacity (Figure 2c), known as *capacity fade*. The percent Coulomb efficiency is as follows:

$$100 Q_{dis}/Q_{ch} \tag{4.0}$$

Additional figures of merit of a rechargeable cell are its density of stored energy, its output power $P(q) = V(q)\, I(q)$ for a given discharge current, its calendar life, and its safety. The density of stored energy in a fully charged cell may be obtained by measuring the time $\Delta t = \Delta t(I_{dis})$ for its complete discharge at a constant current $I_{dis} = dq/dt$:

$$\text{Energy density} = \int_0^{\Delta t} IV(t)\, dt/\text{wt} = \int_0^Q V(q)\, dq/\text{wt} \tag{5.0}$$

where wt is the weight of the cell. This *gravimetric* energy density (W h/kg or mW h/g) is dependent on I_{dis} through

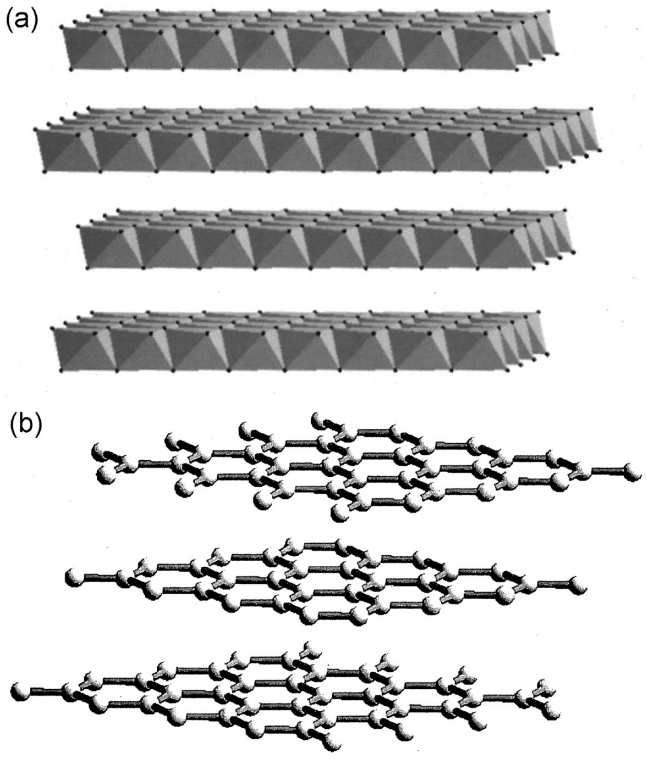

FIGURE 4. Close-packed $MX_{6/3}$ layers; interlayer bonding by H^+ in NiOOH; van der Waals bonds in TiS_2; Li^+ in $LiCoO_2$.

$Q(I_{dis})$. The *volumetric* energy density (W h/L) is of particular interest for mobile batteries, particularly those that power hand-held or laptop devices.

The electrolyte of a cell may be a crystalline solid, a glass, a polymer, or a liquid. With solid electrodes, a liquid or polymer electrolyte is preferred, since it is difficult to retain a close solid–solid electrode–electrolyte interface over many charge–discharge cycles. The energy gap E_g between the lowest unoccupied molecular orbital (LUMO) and the highest occupied molecular orbital (HOMO) of a liquid electrolyte is the *window* of the electrolyte. As illustrated in Figure 3, the electrochemical potentials μ_A and μ_C of the anode and the cathode of a charged cell need to be matched to the LUMO and HOMO of the electrolyte for maximum $V(q)$ of a stable cell. If the μ_A, i.e. Fermi energy of a solid anode, is above the LUMO of the electrolyte, the anode will reduce the electrolyte; and if the μ_C of a cathode is below the HOMO of the electrolyte, the cathode will oxidize the electrolyte unless the energy of electron transfer across an interface provides a *kinetic stability*; but normally, formation of a solid-electrolyte interphase (SEI) passivation layer by an electrode–electrolyte chemical reaction is needed to stabilize a mismatched electrode.[3] Moreover, the SEI layer must be electronically insulating and permeable to the working ion.

Cells containing solid electrodes normally have liquid or elastic-polymer electrolytes. Solid electrolytes are used with liquid electrodes; a gaseous cathode encounters a liquid electrolyte. We distinguish cells that use a liquid or polymer electrolyte from those that use a solid electrolyte.

3. Aqueous Electrolytes

Traditional rechargeable batteries use an acidic, e.g. H_2SO_4, or an alkaline, e.g. KOH, aqueous electrolyte having a proton conductivity $\sigma_H \simeq 1$ S cm^{-1}. However, an aqueous electrolyte has a window between its LUMO and its HOMO of only 1.23 eV, which means that the maximum stable open-circuit voltage for a long shelf life is $V_{oc} \simeq 1.5$ V.

The cathode $Ni(OH)_{2-x}O_x$ ($0 \leq x \leq 1$) allows *reversible intercalation* of H^+ ions between the O–Ni–O close-packed layers of Figure 4; the electrons operate on the Ni^{3+}/Ni^{2+} redox couple. (*Note*: the superscripts on ions are used as a convenient label; they do not represent the actual charge on the ion.) Intercalation of the working ion between close-packed MO_2 layers of a transition-metal compound is a two-dimensional (2D) example of a *reversible insertion reaction*. In a metal-hydride MH_x anode, the H^+ ion is inserted reversibly into a 3D interstitial space where it is charge-compensated by formation of the metal hydride.

A *reversible displacement* reaction is also possible; it occurs at the traditional Cd and Pb anodes as

$$Cd^0 + 2H_2O = Cd(OH)_2 + 2H^+ + 2e^- \qquad (6.1)$$

$$Pb^0 + H_2SO_4 = Pb(SO)_4 + 2H^+ + 2e^- \qquad (6.2)$$

in the rechargeable $Ni(OH)_2$/KOH/Cd (nickel–cadmium) and PbO_2/H_2SO_4/Pb (lead-acid) batteries. The nickel–cadmium cell has a stable $V_{oc} = 1.5$ V, but the $V_{oc} = 2.0$ V of the lead-acid battery has a limited shelf life owing to a slow, irreversible precipitation of solid $PbSO_4$. In these two examples, the large volume change associated with the reversible displacement reaction at the anode occurs at the surface of a metallic plate, where it can be accommodated in the liquid electrolyte.

4. Solid β,β''- Alumina Electrolyte[1,4]

The discovery in 1967 of fast 2D Na^+-ion transport in β-Al_2O_3 by Kummer and Weber[5] at the Ford Motor Co. and their suggestion of the S/β-Al_2O_3/Na (sodium–sulfur) battery opened the door to consideration of nonaqueous electrolytes.

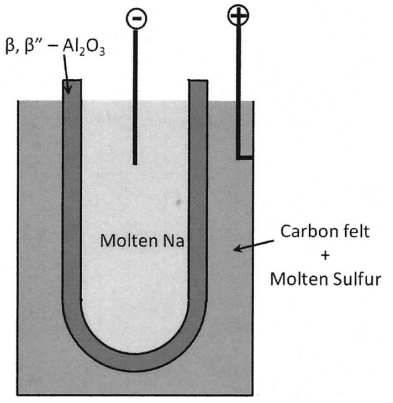

FIGURE 5. Schematic of a S/Na cell with a Na^+-ion electrolyte tube.

The sodium–sulfur battery (Figure 5) uses molten sodium as the anode, molten sulfur impregnated with a porous, soft-carbon felt as the cathode, and a thin β,β''-Al_2O_3 composite-solid membrane as both electrolyte and separator; it operates at 300–350 °C with a $V_{oc} \approx 2.0$ V. The electrode reactions are as follows:

Anode:

$$2Na^0 = 2Na^+ + 2e^- \qquad (7.1)$$

Cathode:

$$S + xNa^+ + xe^- = Na_x\ S \text{ on carbon} \qquad (7.2)$$

The sodium–sulfur battery is now operational in Japan.[6] Its development had two immediate consequences: it stimulated (1) a search for oxide framework structures that would support 3D Na^+-ion conductivity[7] and (2) consideration of molten-salt cathodes in place of sulfur,[8] e.g.

$$2Na + NiCl_2 = 2NaCl + Ni \qquad (8.0)$$

to give a higher $V_{oc} = 2.58$ V at 350 °C. The $NiCl_2/\beta,\beta''$-Al_2O_3/ Na cell is referred to as the *Zebra battery*.

The sodium–sulfur battery has also opened the door to consideration of other high-temperature battery configurations, viz. a gaseous fuel-cell/electrolysis-cell cycle via an Fe/FeO_x oxidation/reduction, based on the solid-oxide fuel-cell technology.[9]

5. Organic Liquid-Carbonate Electrolytes[10]

A nonaqueous liquid electrolyte with a larger LUMO–HOMO energy gap would enable design of a room-temperature cell with a higher voltage, but the only known liquid in which H^+ ions are mobile is water. However, Li salts dissociate in

organic liquid-carbonate solvents, and those aprotic Li^+ electrolytes, if containing an ethylene carbonate (EC) additive, form a passivating solid-electrolyte-interphase (SEI) layer on a lithium anode. The availability of a liquid nonaqueous electrolyte stable against lithium appeared to open up the possibility of a Li-ion rechargeable battery, provided a suitable solid cathode could be found.

Given the reversible intercalation of H^+ ions into a NiOOH cathode and the pioneering work on Li intercalation into layered transition-metal sulfides by Robert Schöllhorn[11] in Germany and Jean Rouxel[12] in France, intercalation of Li into layered TiS_2 was suggested as a viable cathode for a rechargeable Li-ion battery. The layered TiS_2 has van der Waals bonding, rather than hydrogen bonding between the TiS_2 layers; see Figure 4. In 1976, Whittingham[13] reported a rechargeable TiS_2/Li cell having excellent rate capability with a $V_{oc} \cong 2.2$ V. However, recharging the cell gives a mossy Li deposit on the anode, and on repeated cycles, a dendrite growth from the anode across the electrolyte can short-circuit the cell with explosive or incendiary consequences.[14] Since a safe alternative anode would lower the voltage to where the Li-ion battery would not be competitive with aqueous-electrolyte rechargeable batteries or a Zebra battery, the intensive effort on Li-ion rechargeable batteries with sulfide cathodes was abruptly abandoned.

Since the energy of the top of the S-3p bands limits the voltage of these sulfide cathodes to below 2.6 V versus lithium, I decided to explore a reversible Li extraction from a layered $LiMO_2$. My group at Oxford reported a reversible removal of Li from $LiCoO_2$ at a voltage $V_{oc} \cong 4.0$ V versus lithium[15,16] and showed that the Li-ion diffusivity in the oxides was even higher than that in the sulfides.[17]

Meanwhile, intercalation of Li into graphitic carbons was being explored by chemists in several countries.[18] Rachid Yazami[19] noted that reversible intercalation of Li into graphitic carbon at a $V_{oc} \cong 0.2$ V versus lithium was not plagued by dendrite formation on slow rates of charge. This led Akira Yoshino[20] to make a $LiCoO_2$/C rechargeable Li-ion battery of high energy density that was safe provided the charging voltage was not large enough to plate lithium on the surface of the carbon. This battery was used by the Sony Corp. to market the first cell telephone, a development that launched the wireless revolution.

Reversible extraction of Li is limited to $x \leq 0.55$ in $Li_{1-x}CoO_2$ and to $x \leq 0.8$ in $Li_{1-x}NiO_2$; for larger values at x, O_2 is evolved from the electrode or H^+ is inserted from the electrolyte on further Li extraction.[21] This phenomenon occurs where the μ_C of the cathode is pinned at the top of the O-2p bands; see Figure 6. This phenomenon has been demonstrated for pinning of μ_C at the top of the S-3p bands.[22] It is important to distinguish the limiting reversible voltage imposed by the HOMO of the electrolyte from the intrinsic voltage limit imposed by pinning of μ_C at the top of the anion-p bands, a limit that depends on the structure and composition of the cathode. In addition, a limit for extended cycle life may be imposed by an irreversible reaction of the electrolyte salt with the carbon that is commonly added to the cathode composite to improve the electronic conductivity.[23,24]

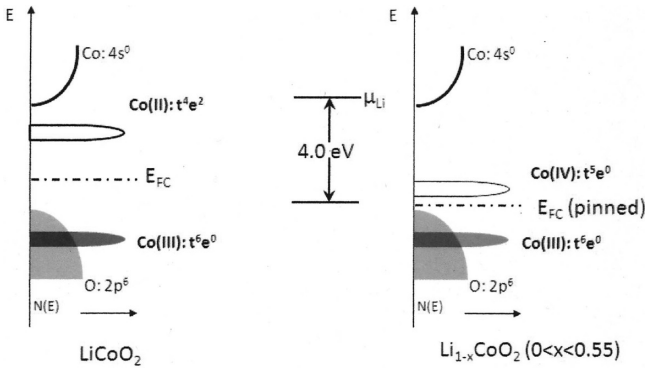

FIGURE 6. Illustration of pinning of μ_C at the top of the O-2p bands as an active cation d^n manifold moves down across the top of the O-2p bands. At a critical O-2p component in the antibonding hole states, surface peroxide ions $(O_2)^{2-}$ are formed.

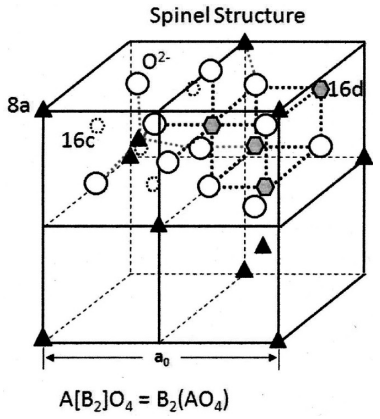

FIGURE 7. Two quadrants of the structure of a cubic $A[B_2]O_4$ spinel.

In 1981, Michael Thackeray came to my laboratory at Oxford to explore the insertion of Li into the less costly oxospinel Fe_3O_4. Since it is not possible to obtain a spinel (see Figure 7), with interstitial cations, we quickly verified from the X-ray data of Bill David[25] that the inserted Li displaced the tetrahedral-site Fe of Fe_3O_4 into neighboring empty octahedral sites to create a rock-salt structure with the

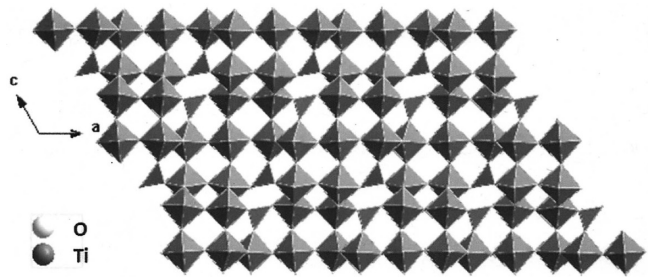

FIGURE 8. Structure of the $TiNb_2O_7$ framework of the anode $Li_xTiNb_2O_7$.

$[Fe_2]O_4$ framework intact. Therefore, I suggested investigation of $Li[Mn_2]O_4$, with the $[Mn_2]O_4$ framework having a 3D interstitial space for Li^+-ion motion. Thackeray subsequently showed that Li insertion gives a $V_{oc} \approx 3.0$ V[26] and Li extraction a $V_{oc} \simeq 4.0$ V[27] versus lithium despite working on the same Mn^{4+}/Mn^{3+} redox couple in the framework. In $Li_{1-x}[Mn_2]O_4$, the Li^+ ions occupy tetrahedral sites, in $Li_{1+x}[Mn_2]O_4$, they occupy octahedral sites. The site shift from tetrahedral to octahedral sites of the Li^+ changes the energy of the Mn^{4+}/Mn^{3+} couple by 1 eV. The one-volt step limits the capacity of the spinels to half a Li per framework cation. Moreover, complications arising from Li^+-ion ordering at $x = 0.5$ as well as from cooperative Jahn–Teller orbital ordering on the Mn^{3+} ions and the surface disproportionation reaction $2Mn^{3+} = Mn^{2+} + Mn^{4+}$ have plagued exploitation of the $V_{oc} \simeq 4.0$ V of a $Li_{1-x}[Mn_2]O_4$ cathode.[28] Nevertheless, a rapid and reversible 3D insertion of Li into the interstitial space of a close-packed oxide-ion framework was established, and Thackeray's group[29] subsequently patented the $Li_{1-x}[Li_{1/3}Ti_{5/3}]O_4$ spinel as a stable anode with a $V_{oc} \simeq 1.5$ V versus lithium, a safe 0.4 V below the LUMO of the organic liquid-carbonate electrolytes.

The energy of the top of the O-2p bands in a layered oxide can be lowered by introducing stronger covalent bonding to a framework cation. Ohzuku[30] of Osaka, Japan, reported accessing two redox couples of Ni, Ni^{4+}/Ni^{3+}, and Ni^{3+}/Ni^{2+}, in the layered oxide $Li(Ni_{0.5}Mn_{0.5})O_2$ at about 4.7 V vs lithium without a significant voltage step between them. Thackeray[31] has pointed out that addition of the layered oxide Li_2MnO_3, i.e. $Li(Li_{1/3}Mn_{2/3})O_2$, allows easier fabrication, but Li_2MnO_3 has an intrinsic voltage limit of 4.5 V.[32] Although a voltage $V_{oc} \simeq 4.7$ V appears possible in this phase and in the spinel $Li_{1-x}[Ni_{0.5}Mn_{1.5}]O_4$,[33] a capacity fade occurs above $V = 4.5$ V.

These observations on oxide cathodes have revealed the following:

(1) Insertion of Li into the interstitial space of a close-packed oxide-ion framework can be rapid. Different frameworks strongly bonded in 3D can also be envisaged;[34] see Figure 8.

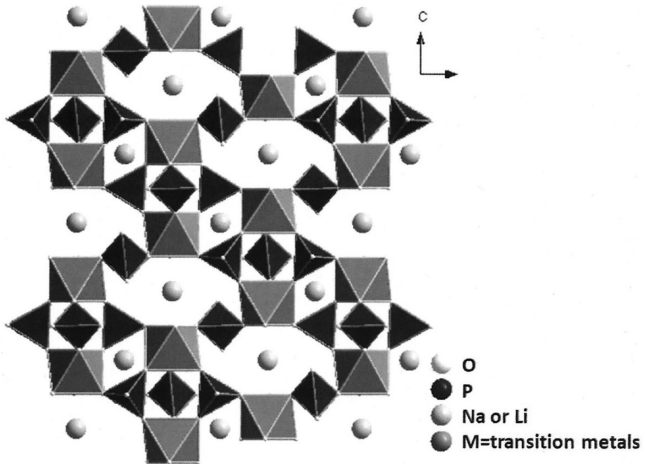

FIGURE 9. NASICON framework structure of hexagonal $Fe_2(SO_4)_3$.

(2) Pinning of the μ_C at the top of the anion-p bands may introduce an intrinsic limit to the voltage obtainable with a cathode. On the other hand, as μ_C approaches the top of the O-2p bands in an oxide cathode, the voltage difference between two successive redox energies may disappear.

(3) Increasing the strength of the covalent components of the anion bonding, as occurs on the isostructural substitution of Mn^{4+} for Ni^{3+} in $Li(Ni_{1-x}Mn_x)O_2$, lowers the energy of the top of O-2p bands to allow realization of a higher cathode voltage.

(4) The specific capacity of a cathode is limited to the number of Li atoms that can be inserted *reversibly* into a framework or layered host per cation of the host. This limited capacity is reduced if, on an initial charge, Li atoms are consumed *irreversibly* in an SEI layer formed on the anode surface.

(5) With an organic liquid-carbonate electrolyte, a safe fast charge requires an anode μ_A at least 0.5 eV below μ_A of lithium, a requirement that can be met with displacement-reaction Li alloys buffered by carbon.[35] However, formation of an SEI layer on an anode with $\mu_A >$ LUMO reduces the limited capacity of an insertion-compound cathode.

6. Oxides Containing Complex Anions $(XO_4)^{n-}$

Frameworks containing $(XO_4)^{n-}$ anions instead of oxide ions can not only open up the interstitial space for fast Li^+-ion or Na^+-ion transport but also provide the strong oxygen covalent bonding needed to lower the top of the O-2p or, with $(XS_4)^{n-}$, the top of the S-3p bands sufficiently to provide a $V_{oc} > 5.0$ V versus lithium. In our earlier search for a framework oxide giving fast 3D Na^+-ion transport,[7] Henry Hong[36]

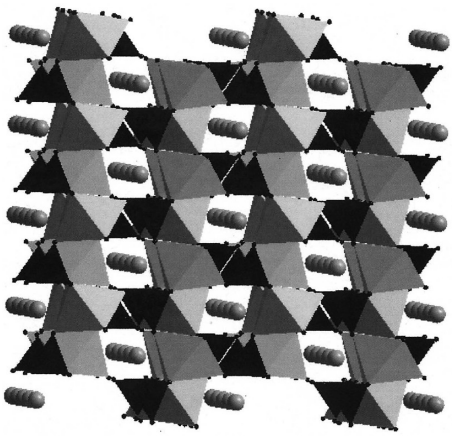

FIGURE 10. $FePO_4$ framework structure showing the 1D tunnels for Li^+-ion motion; motion is blocked if there is a Li, Fe antisite exchange in $LiFePO_4$.

showed that $Na_{1+3x}Zr_2(P_{1-x}Si_xO_4)_3$ with $x = {}^2/_3$ gives a superior Na^+-ion conductivity, which prompted colleagues to call the $M_2(XO_4)_3$ framework of Figure 9 the NASICON structure, standing for NA superionic conductor. Therefore, I suggested exploring Li^+-ion insertion into $Fe_2(XO_4)_3$ frameworks with X = Mo, W, or S. Manthiram showed[37] that the voltage of these compounds jumps from $V_{oc} \approx 3.0$ V with X = Mo or W to 3.6 V versus lithium with X = S. This experiment demonstrated the influence, through the inductive effect, of the countercation X on the Fe^{3+}/Fe^{2+} redox energy. It also prompted use of the NASICON structure to explore, in an isostructural framework, the relative energies of redox couples with $(SO_4)^{2-}$ versus $(PO_4)^{3-}$ complex anions;[38] every redox energy was found to be stabilized by about 0.8 eV on changing from $(PO_4)^{3-}$ to $(SO_4)^{2-}$. In the course of this work, my student Ashoka Padhi,[39] aided by my postdoc Kirakodu Nanjundaswamy, discovered reversible Li insertion at a $V_{oc} = 3.45$ V versus lithium in the $FePO_4$ framework of the ordered olivine $LiFePO_4$ (Figure 10). The group of Michel Armand,[40] who was then at the University of Montreal, Canada, subsequently showed that preparation of $LiFePO_4$ from $FePO_4$ particles in a reducing carbon atmosphere gives full capacity at high charge/discharge rates. The voltage of this carbon-coated cathode lies within the window of the electrolyte, and workers with Karim Zaghib of the Hydro Quebec Corp. have shown it can provide a safe, high-power battery with a long cycle life.[41] Yet Ming Chiang of MIT has marketed successfully batteries with $LiFePO_4$ cathodes for power tools and small electric vehicles through his A123 Corp.

Although these studies have resulted in a worldwide race to develop safe power batteries of long cycle life for electric vehicles and electrical energy storage, a strategy based on Li-insertion cathodes, an anode of carbon-buffered Li alloy or $Li_4Ti_5O_{12}$ spinel, and an organic liquid-carbonate electrolyte is facing a frustrating limitation on the capacity of the individual cell. A discharged carbon-buffered S cathode, $C-Li_2S$, represents an alternative to an oxide insertion compound that can be used with a gel electrolyte,[42] but this cathode needs to be used with a lithium anode.

Lithium Solid Electrolytes as Separators. The introduction of a solid electrolyte with a conduction band above and a valence band over 5 eV below the μ_A of a lithium anode would allow use of a high-voltage cathode and a lithium anode without an irreversible Li loss from the cathode in an anode SEI layer on the first charge. Elimination of the irreversible Li loss from the cathode would increase the capacity even with Li-insertion cathodes. However, this strategy requires identification of a suitable Li^+-ion solid electrolyte.

The volume changes of insertion-compound solid electrodes on charge/discharge cycling make it unlikely that all-solid-state batteries of long cycle life and large capacity can be realized. However, we can envisage a battery containing a Li^+-ion solid-electrolyte separator with two different liquids on either side contacting a lithium anode on one side and an aqueous solution on the other side; this configuration would allow replacing the capacity-limiting insertion-compound cathodes with other strategies.

The conventional flow-through battery has different redox couples in aqueous solution as anode and cathode separated by an H^+-permeable membrane; it is being explored[1,43] as a large-capacity battery, but the NAFION-based membranes are expansive and short-lived; also, redox couples leak across them. An alternative is to have a solid Li^+ electrolyte as separator with only the cathode operating in the flow-through mode. Yuhao Lu[44] has demonstrated the feasibility of this concept; with the $Fe(CN)_6{}^{3-}/Fe(CN)_6{}^{4-}$ redox couple in a flow-through alkaline solution as cathode, he has shown a reversible $V_{oc} = 3.45$ V with excellent Coulomb efficiency. Y.-M. Chiang of MIT[45] has formed a company to explore an active-particle flow-through cathode.

The Li/air battery, which uses gaseous O_2 as the cathode, has also been proposed as a large-capacity alternative;[46] it relies on two catalytic reactions at the cathode, an oxygen reduction reaction (ORR) on discharge, and an oxygen-evolution reaction (OER) on charge. The efficiency of electrical energy storage with this battery is low because the two reactions occur at different potentials. Moreover, an interesting voltage requires an anode with a μ_A close to that

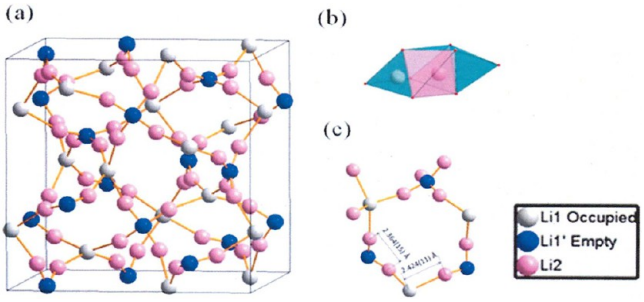

FIGURE 11. (a) $A_3B_3C_2O_{12}$ cubic garnet structure, which contains a $B_3C_2O_{12}$ framework with a 3D interconnected interstitial space of tetrahedral A sites bridged by an octahedral site. (b) The displacement of a Li^+ ion in a bridging octahedral site having only one of its two neighboring tetrahedral sites occupied by a Li^+ ion (after O'Callaghan and Cussen).[53] (c) Interstitial space with ideal ordering of tetrahedral-site vacancies for 7.5 Li^+ ions.

of lithium. The cathode does not cycle in an organic liquid-carbonate electrolyte;[47] but it can cycle with only a 0.3 V separation between discharge and charge voltages in an aqueous solution. This performance has been demonstrated with a single bifunctional catalyst.[48] A similar result has been obtained by using two different catalysts.[49] In each case, the cell consisted of a lithium anode in a liquid-carbonate electrolyte separated from an aqueous solution on the cathode side by a Li^+-ion solid electrolyte.

The challenge for these strategies is to identify a Li^+ electrolyte stable both on contact with lithium and with an alkaline aqueous solution as well as having a room-temperature $\sigma_{Li} > 10^{-3}$ S cm^{-1}. The strong covalent bonding in $(XS_4)^{n-}$ complex anions provides a large enough electrolyte window, and sulfide glasses are known[50] to give a room temperature $\sigma_{Li} > 10^{-3}$ S cm^{-1}; but if an aqueous alkaline solution is to be used, an oxide Li^+-ion solid electrolyte would seem to be required. The recent report[51] of a room-temperature $\sigma_{Li} = 1.2 \times 10^{-2}$ S cm^{-1} in $Li_{10}GeP_2S_{12}$ and its use in an all-solid cell deserves a critical evaluation. The garnet framework (Figure 11) of $Li_{7-x}La_3Zr_{2-x}Ta_xO_{12}$ offers an oxide Li^+-ion electrolyte with a room-temperature $\sigma_{Li} \simeq 10^{-3}$ S cm^{-1} for a nominal $0.4 \leq x \leq 0.6$.[52]

Until the problems with strategies for alternative large-capacity cathodes are resolved, industry will continue with efforts to increase safety and, at lower cost, the energy density and cycle life of Li-ion power batteries having insertion-compound cathodes. Fundamental studies of materials chemistry and electrode morphologies will continue to create alternative battery strategies.

This work was supported by the Assistant Secretary for Energy Efficiency and Renewable Energy, Office of Vehicle Technologies, U.S. Department of Energy, under Contract DE-AC02-05CH11231 through the Batteries for Advanced Transportation Technologies (BATT) Program Subcontract 6805919. The work was also supported by the Robert A. Welch Foundation of Houston, TX.

BIOGRAPHICAL INFORMATION

John B. Goodenough joined the Cockrell School of Engineering in 1986, on retirement from the University of Oxford, England. Before going to England, he spent 24 years at the MIT Lincoln Laboratory as a Group Leader and Research Scientist. He has authored two books and coauthored one. He is a member of the National Academy of Engineering and of the National Academy of Sciences, and a foreign associate of the Academy of Sciences of France, Spain, and England. Among other awards, he received the prestigious Japan Prize in 2001 and the Presidential Enrico Fermi Award in 2009.

Dr. Goodenough studies the relationships between the chemistry, structure, and electrical properties of solids in order to design new or improved technical materials. With Professor Jianshi Zhou, he uses high pressure to study the unusual physical properties encountered at the transition from magnetic to metallic behavior in transition-metal oxides. His research interests are focused in the following three areas: (1) Magnetism: In the 1950s, while helping to develop the magnetic memory element of the first random-access memory (RAM) of the digital computer with a ferrimagnetic ceramic, Goodenough developed the rules for the sign, ferromagnetic versus antiferromagnetic, of interatomic spin−spin interactions, now known as the Goodenough−Kanamori rules, and the role of cooperative orbital order−disorder transitions. See his book *Magnetism and the Chemical Bond*. (2) Localized versus Itinerant Electronic Behavior: His long review *Metallic Oxides*, translated as the book *Les oxides des métaux de transition*, chronicles his pioneering investigations into the transitions among d electrons in transition metal oxides from itinerant behavior, as in metallic TiO and $LaNiO_3$, to localized behavior, in MnO and $LaFeO_3$. He continues these investigations with high pressure as well as temperature as variables. (3) Electrochemical Energy Storage and Conversion: Interrupted by the first energy crisis and a move to the University of Oxford, England, he has used his experience with oxides to develop electrodes and solid electrolytes for rechargeable batteries and for the solid oxide fuel cell.

FOOTNOTES

*E-mail: jgoodenough@mail.utexas.edu.
The authors declare no competing financial interest.

REFERENCES

1 Yang, Z.; Zhang, J.; Kintner-Meyer, M. C. W.; Lu, X.; Choi, D.; Lemmon, J. P.; Liu, J. Electrochemical Energy Storage for Green Grid. *Chem. Rev.* **2011**, *111*, 3577–3613.

2 Winter, M.; Brodd, R. T. What are Batteries, Fuel Cells, and Supercapacitors? *Chem. Rev.* **2004**, *104*, 4245–4269.

3 Fong, R.; von Sacken, V.; Dahn, J. R. Studies of Lithium Intercalation into Carbons Using Nonaqueous Electrochemical Cells. *J. Electrochem. Soc.* **1990**, *137*, 2009–2013.

4 Lu, X.; Xia, G.; Lemmon, J. P.; Yang, Z. Advanced materials for sodium-beta alumina batteries: status, challenges, and perspectives. *J. Power Sources* **2010**, *195*, 2431–2442.

5 Kummer, J. T.; Weber, N. U.S. Patent 3,413,150, 1968.

6 Roth, W. L.; Reidinger, F.; LaPlaca, S. Studies of Stabilization and Transport Mechanisms in Beta and Beta′′ Alumina by Neutron Diffraction. In *Superionic Conductors*; Mahan, G. D., Roth, W. L., Eds.; Plenum Press: New York, 1976; pp 273−241.

7 Goodenough, J. B.; Hong, H. Y.-P.; Kafalas, J. A. Fast Na^+-ion Transport in Skeleton Structures. *Mater. Res. Bull.* **1976**, *11*, 203–220.

8 Coetzer, J.; New High, A. Energy Density Battery System. *J. Power Sources* **1986**, *18*, 377–380.

9 Xu, N.; Li, X.; Zhao, X.; Goodenough, J.B.; Huang, K. A Novel Battery for Grid Energy Storage. (to be published).

10 Xu, K. Nonaqueous Liquid Electrolytes for Lithium-Based Rechargeable Batteries. *Chem. Rev.* **2004**, *10*, 4303–4417.

11 Schöllhorn, R. Solvated Intercalation Components of Layered Chalcogenide and Oxide Bronzes. In *Intercalation Chemistry*; Whittingham, M. S., Jacobson, A. J., Eds.; Academic Press: New York, 1982; pp 315−360.

12 Rouxel, J. In *Intercalated Layered Materials*; Levy, F., Ed.; Reidel Publishing: Dordrecht, Netherlands, 1979; pp 201−250.

13 Whittingham, M. S. Electrical Energy Storage and Intercalation Chemistry. *Science* **1976**, *192*, 1126–1127.

14 Aurbach, D.; Gofer, Y.; Langsam, J. The Correlation Between Surface Chemistry, Surface Morphology, and Cycling Efficiency of Lithium Electrodes in a Few Polar Aprotic Systems. *J. Electrochem. Soc.* **1989**, *136*, 3198–3205.

15 Mizushima, K.; Jones, P. C.; Wiseman, P. J.; Goodenough, J. B. Li_xCoO_2 ($0 < x \leq 1$): A New Cathode Material for Batteries of High Energy Density. *Mater. Res. Bull.* **1980**, *15*, 783–789.

16 Goodenough, J. B.; Mizushima, K.; Takeda, T. Solid-solution Oxides for Storage-Battery Electrodes. *Jpn. J. Appl. Phys.* **1980**, *19* (Supplement 19-3), 305–313.

17 Thomas, M. G. S. R.; Bruce, P. G.; Goodenough, J. B. Lithium Mobility in the Layered Oxide $Li_{1-x}CoO_2$. *Solid State Ionics* **1985**, *17*, 13–19.

18 Bartlett, N.; McQuillan, B. W. Graphite Chemistry. In *Intercalation Chemistry*, Whittingham, M. S., Jacobson, A. J., Eds.; Academic Press: New York, 1982; pp 19−53.

19 Yazami, R.; Touzain, Ph. A Reversible Graphite-Lithium Negative Electrode for Electrochemical Generators. *J. Power Sources* **1983**, *9*, 365–371.

20 Yoshino, A. U.S. Patent No. 4,688,595 and JP No. 1989293, 1985.

21 Chebiam, R. V.; Prado, F.; Manthiram, A. Soft Chemistry Synthesis and Characterization of Layered $Li_{1-x}Ni_{1-y}Co_yO_{2-\partial}$ ($0 \leq x \leq 1$ and $0 \leq y \leq 1$). 2001, *13*, 2951−2957.

22 Goodenough, J. B.; Kim, Y. Challenges for Rechargeable Li Batteries. *Chem. Mater.* **2010**, *22*, 587–603.

23 Märkle, W.; Colin, J. F.; Goers, D.; Spahr, M. E.; Novak, P. In Situ X-Ray Diffraction Study of Different Graphites in a Propylene Carbonate Based Electrolyte at Very Positive Potentials. *Electrochim. Acta* **2010**, *55*, 4964–4969.

24 Edström, K.; Gustafsson, T.; Thomas, J. O. The Cathode-Electrolyte Interface in the Li-ion Battery. *Electrochim. Acta* **2004**, *50*, 397–403.

25 Thackeray, M. M.; David, W. I. F.; Goodenough, J. B. Structural Characterization of the Lithiated Iron Oxides $Li_xFe_3O_4$ and $Li_xFe_2O_3$ ($0 < x < 2$). *Mater. Res. Bull.* **1982**, *17*, 785–793.

26 Thackeray, M. M.; David, W. I. F.; Bruce, P. G.; Goodenough, J. B. Lithium Insertion into Manganese Spinels. *Mater. Res. Bull.* **1983**, *18*, 461–472.

27 Thackeray, M. M.; Johnson, P. J.; de Picciotto, L. A.; Bruce, P. G.; Goodenough, J. B. Electrochemical Extraction of Lithium from $LiMn_2O_4$. *Mater. Res. Bull.* **1984**, *19*, 179–187.

28 Shin, Y.; Manthiram, A. Influence of Lattice Parameter Difference between the Two Cubic Phases Formed in the 4 V Region on the Capacity Fading of Spinel Manganese Oxides. *Chem. Mater.* **2003**, *15*, 2954–2961.

29 Ferg, E.; Gummow, R. J.; de Kock, A.; Thackeray, M. M. Spinel Anodes for Lithium-ion Batteries. *J. Electrochem. Soc.* **1994**, *141*, L147–L150.

30 Makimura, Y.; Ohzuku, T. Lithium Insertion Material of $LiNi_{1/2}Mn_{1/2}O_2$ for Advanced Lithium-ion Batteries. *J. Power Sources* **2003**, *117*, 156–160.

31 Rousouw, M. H.; Liles, D. C.; Thackeray, M. M. Synthesis and Structural Characterization of a Novel Layered Lithium Manganese Oxide, $Li_{0.36}Mn_{0.91}O_2$, and its Lithiated Derivative, $Li_{1.09}Mn_{0.91}O_2$. *J. Solid State Chem.* **1993**, *104*, 464–466.

32 Soon, J.; Goodenough, J. B. (unpublished).

33 Hassoun, J.; Reale, P.; Panero, S.; Scrosati, B.; Wachter, M.; Fleischhammer, M.; Kasper, M.; Wohlfarht-Mehrens, M. Determination of the Safety Level of an Advanced Lithium Ion Battery having a Nanostructural Sn-C anode, a High-Voltage $LiNi_{0.5}Mn_{1.5}O_4$ Cathode, and a Polyvinylidene Fluoride-Based Gel Electrolyte. *Electrochem. Acta* **2010**, *55*, 4194–4200.

34 Han, J.; Goodenough, J. B. 3-V Full Cell Performance of Anode Framework $TiNb_2O_7$/Spinel $LiNi_{0.5}Mn_{1.5}O_4$. *Chem. Mater.* **2011**, *23*, 3404–3407.

35 Yoon, S.; Manthiram, A. Sb-MO_x-C (M = Al, Ti, or Mo) Nanocomposite Anodes for Lithium-Ion Batteries. *Chem. Mater.* **2009**, *20*, 3898–3904.

36 Hong, H. Y.-P. Crystal Structures and Crystal Chemistry in the System $Na_{1+x}Zr_2Si_xP_{3-x}O_{12}$. *Mater. Res. Bull.* **1976**, *11*, 173–182.

37 Manthiram, A.; Goodenough, J. B. Lithium Insertion into $Fe_2(SO_4)_3$ Frameworks. *J. Power Sources* **1989**, *26*, 403–408.

38 Padhi, A. K.; Nanjundaswamy, K. S.; Masquelier, C.; Goodenough, J. B. Mapping of Transition-Metal Redox Couples in Phosphates with NASICON structure by Lithium Intercalation. *J. Electrochem. Soc.* **1997**, *144*, 2581–2586.

39 Padhi, A. K.; Nanjundaswamy, K. S.; Goodenough, J. B. Phospho-Olivines as Positive Electrode Materials for Rechargeable Lithium Batteries. *J. Electrochem. Soc.* **1992**, *144*, 1188–1194.

40 Ravet, N.; Goodenough, J. B.; Besner, S.; Simoneau, M.; Hovington, P.; Armand, M. Improved Iron Based Cathode Material. *196th Electrochemical Society Meeting*, Honolulu, HI, 1999.

41 Zaghib, K.; Mauger, A.; Goodenough, J. B.; Julien, C. M.Design and Properties of $LiFePO_4$ Nanomaterials for High Power Applications. In *Nanotechnology for Li-ion Batteries*; Lockwood, D., Ed.; Springer Verlag: Berlin, 2011; Chapter 8.

42 Massoun, J.; Scrosati, B. A High-Performance Polymer Tin Sulfur Lithium Ion Battery. *Angew. Chem.* **2010**, *49*, 2371–2374.

43 Rychcik, M.; Skyllas-Kazacos, M. Characteristics of a New All-Vanadium Redox Flow Battery. *J. Power Sources* **1988**, *23*, 59–67.

44 Lu, Y.; Goodenough, J. B. Rechargeable alkali-ion cathode-flow battery. *J. Mater. Chem.* **2011**, *21*, 10113–10117.

45 Duduta, M.; Ho, B.; Wood, V. C.; Limthongkul, P.; Brunini, V. E.; Carter, W. C.; Chiang, Y.-M. Semi-Solid Lithium Rechargeable Flow Battery. *Adv. Energy Mater.* **2011**, *1*, 511–516.

46 Abraham, K. M.; Jiang, Z. A Polymer Electrolyte-Based Rechargeable Lithium/Oxygen Battery. *J. Electrochem. Soc.* **1996**, *143*, 1–5.

47 Freunberger, S. A.; Chen, Y.; Peng, Z.; Griffin, J. M.; Hardwick, L. J.; Bardé, F.; Novak, P.; Bruce, P. G. Reaction in the Rechargeable Lithium-O_2 Battery with Alkyl Carbonate Electrolytes. *J. Am. Chem. Soc.* **2011**, *133*, 8040–8047.

48 Wang, L.; Goodenough, J. B. (to be published).

49 Li, L.; Pan, J.; Fu, Y.; Manthiram, A. (to be published).

50 Mayashi, A.; Minami, K.; Mizuno, F.; Tatsumisago, M. Formation of Li^+ superionic crystals from the Li_2S-P_2S_5 Melt-Quenched glasses. *J. Mater. Sci.* **2008**, *43*, 1885–1889.

51 Kamaya, N.; Homma, K.; Yamakawa, Y.; Hirayama, M.; Kanno, R.; Yonemura, M.; Kamiyama, T.; Kato, Y.; Hama, S.; Kawamoto, K.; Mitsui, A. A Lithium Superionic Conductor. *Nat. Mater.* (in press).

52 Li, Y.; Goodenough, J. B. (to be published).

53 O'Callaghan, M. P.; Cussen, E. J. Lithium Dimer Formation in the Li-Conducting Garnets $Li_{5+x}Ba_xLa_{3-x}Ta_2O_{12}$ ($0 < x < 0.16$). *Chem. Commun.* **2007**, 2048–2050.

Note Added after ASAP Publication This paper was published on the Web on July 2, 2012. Additional changes were made throughout, and the corrected version was reposted on July 9, 2012.